South East Asian J. of Mathematics and Mathematical Sciences
Vol. 22, No. 1 (2026), pp. 295-322

DOI: 10.56827/SEAJMMS.2026.2201.19 **ISSN (Online): 2582-0850**

ISSN (Print): 0972-7752

SHOCK WAVE PROPAGATION IN A SELF-GRAVITATING DUSTY GAS WITH MAGNETIC FIELD IN A ROTATING MEDIUM

Ritika Omar and G. Nath

Department of Mathematics,
Motilal Nehru National Institute of Technology, Allahabad
Prayagraj - 211004, Uttar Pradesh, INDIA

E-mail : ritika.2023rma54@mnnit.ac.in, gnath@mnnit.ac.in

(**Received:** *Dec. 10, 2025* **Accepted:** *Dec. 20, 2025* **Published:** *Apr. 30, 2026)*

Abstract: This study investigates the propagation of exponential shock wave in a self-gravitating, rotating, perfectly conducting mixture of perfect gas and small solid particles (dusty gas) subjected to an axial or azimuthal magnetic field for both the adiabatic and isothermal flow conditions. The analysis incorporates the components of the vorticity vector, and both the isothermal and adiabatic compressibilities. In the present model, the solid particles are assumed to be continuously dispersed throughout the mixture, and flow equilibrium is maintained across the entire flow-field region behind the shock front. The impact of the variations in the physical parameters of the problem on the flow behavior is also investigated. It is worth to notice that, due to an increase in the gravitational parameter or the ratio of the solid-particle density to the initial gas density, the strength of the shock wave increases, while an increment in the adiabatic index or the shock Cowling number results reduction in the shock strength. The presence of an axial magnetic field enhances the shock strength in comparison to that of azimuthal magnetic field. Also, the shock wave is weaker in the isothermal flow condition as compared to the adiabatic flow condition.

Keywords and Phrases: Self-similar solution, shock waves, magnetogasdynamics, dusty gas, rotating medium, adiabatic and isothermal flows.

2020 Mathematics Subject Classification: 76L05, 76L20, 76M55, 76T05, 76U05, 76W05.

1. Introduction

Shock waves constitute a critical phenomenon in both fundamental and applied physics, arising in diverse domains such as aerodynamics and hydrodynamics, as well as in extreme-energy environments exemplified by inertial confinement fusion, supernova explosions, and underwater electrical discharges of wires and wire arrays (see Chefranov, S. G. [7]). Supersonic astrophysical flows endowed with angular momentum often give rise to the formation of shock waves. In recent years, the investigation of shock waves that arise in rotating transonic and supersonic astrophysical fluid flows has gained critical importance. Chaturani (see Chaturani, P. [6]) has investigated the propagation of cylindrically symmetric shock waves in a gas undergoing solid-body rotation and derived solutions using the similarity technique originally proposed by Sakurai (see Sakurai, A. [41]). Levin and Skopina (see Levin, V. A. and Skopina, G. A. [19]) have examined the detonation wave propagating into a rotating gaseous medium. Several other notable contributions on shock waves into a rotating gaseous medium can be found in (see Nath, G. [22], Nath, G. [23], Nath, G. and Maurya, A. [24]).

The analysis of shock-wave propagation in a gas laden with micron-sized solid particles is of considerable importance due to its wide range of practical application such as nozzle flows, underground explosions, lunar dust transport. In addition, particle acceleration by shocks, dusty crystal formation, and several other engineering and astrophysical problems are closely associated with this type of flow (see Popel, S. I. amd Gisko, A. A. [33], Miura, H. and Glass, I. I. [20]). Pai et al. (see Pai, S. I., Menon, S. and Fan, Z. Q. [30]) have generalized the problem of a strong explosion generated by a rapid energy release in gas (see Sedov, L. I. [43], Korobeinikov, V. P. [15]) by extending it to a dusty gas (a mixture of perfect gas and small solid particles).

It is well established that shock waves substantially increase the temperature of a gas to extremely high levels, leading to ionization (see Greenspan, H. P. [11], Chu, C. K. [9], Christer, A. H. [8]). Consider the infinite electrical conductivity under the assumption that the magnetic field is permeated initially and the interaction between magnetic field and the fluid is stronger, and the magnetic field is 'frozen' in the fluid. The assumption of infinite electrical conductivity (perfect conductivity) can be justified because the gas is highly ionized by the shock waves, resulting in a very high electrical conductivity. The case of high electrical conductivity may be well approximated by the limiting case of infinite electrical conductivity, more exactly, infinite magnetic Reynold's number (see Sakurai, A. [42]). Consequently, electromagnetic interactions become essential in the analysis of shock wave propagation. Magnetic fields are widely regarded as having a profound influence on

the dynamics of all astrophysical plasmas, including the dynamo processes, plasma dynamics in clusters, stars, and galaxies. Many other astrophysical processes are also strongly influenced by the presence of magnetic fields (see Hartmann, L. [13], Blandford, R. and Eichler, D. [4]).

The self-gravitating gaseous medium plays a crucial role in the formation of stars and galaxies, as well as in the rapid expansion caused by instantaneous line explosions (see Penston, M. V. [32], Truelove, J.K. et al. [46]). Observational evidence further indicates that the unsteady motion of a massive gaseous body, followed by an instantaneous energy release, triggers flare-like phenomena such as novae and supernovae. The overall behavior of such gaseous masses can be qualitatively understood by examining the equations governing motion and equilibrium while incorporating gravitational effects (see Nath, G. and Singh, S. [25]). In the works of Sedov (see Sedov, L. I. [43]) and Carrus (see Carrus, P. A. [5]), the numerical solutions for a self-gravitating gas under isothermal flow conditions have been obtained.

Rao and Ramana (see Rao, M. P. R. and Ramana, B. V. [37]) have investigated one-dimensional self-similar unsteady flow of a perfect gas behind a strong exponential shock driven out by a piston moving with time according to an exponential law. Vishwakarma and Nath (see Vishwakarma, J. P. and Nath, G. [47]) have investigated the propagation of exponential shock waves in a dusty gas, consisting of perfect gas and small solid particles. They have considered both the adiabatic and isothermal flows for cylindrical and spherical symmetries without taking the effects of rotation, gravitation, and magnetic fields. They have derived the similarity and numerical solutions for strong shock wave. In Nath (see Nath, G. [22]), the author has explored the similarity solutions for the same problem studied by Vishwakarma and Nath (see Vishwakarma, J. P. and Nath, G. [47]) in rotating medium by taking vorticity vector and its components. Nath (see Nath, G. [26]) has generalized the problem studied by Vishwakarma and Nath (see Vishwakarma, J. P. and Nath, G. [47]) for non-ideal dusty gas with magnetic field under the assumption that the dusty gas is the mixture of perfectly conducting non-ideal gas and micro size small solid particles under the assumption of charging of dust particles for the applicability of hydrodynamic model, while in (see Vishwakarma, J. P. and Nath, G. [47]) dusty gas is taken as non-conducting mixture of perfect gas and chemically inert small solid particles. Also, Nath (see Nath, G. [27]) has generalized the problem studied by Nath (see Nath, G. [22]) by considering dusty gas to be the mixture of self-gravitating non-ideal gas and small solid particles instead of mixture of perfect gas and small solid particles in rotating medium, while in (see Nath, G. [22], Vishwakarma, J. P. [47], Nath, G. [26]) the gas is considered as non-gravitating in

rotating or non-rotating medium with or without magnetic field.

In this study, we extended the work done by Vishwakarma and Nath (see Vishwakarma, J.P. and Nath, G. [47]) for ideal gas, to the self-gravitating mixture of ideal gas and small solid particles with the magnetic field into a rotating medium. Also, our work is the generalization of the work of Nath (see Nath, G. [22]), by considering the effect of magnetic field and gravitation; or the work of Nath (see Nath, G. [26]) by considering the effect of magnetic field for perfectly conducting mixture of perfect gas and small solid particles. The shock wave is considered to be generated by the moving cylindrical piston, whose motion follows an exponential time dependence law described as follows

$$x_p = I_0 \exp(lt); \quad l > 0, \tag{1}$$

where x_p denotes the piston radius, t is the time, I_0 and l are constants with dimension. Here, 'I_0' corresponds to the piston's initial radius (see Nath, G. [22], Vishwakarma, J. P. [47]).

The piston motion law given in Eq. (1) prescribes the boundary condition for the speed of the gas at the surface of the piston, which plays a crucial role in defining the problem. Since the aim of the present analysis is to analyze the self-similar flow behavior, it is therefore reasonable to postulate

$$x_s = K_0 \exp(lt), \tag{2}$$

where x_s denotes the shock front radius, and K_0 denotes the constant with dimension (see Nath, G. [22], Vishwakarma, J. P. [47]).

A powerful explosion gives rise to a strong shock wave, and the elevated flow temperatures lead to significant radiative heat transfer behind the strong shock fronts. For flows of this nature, the assumption of adiabatic flow is no longer applicable. Hence, an approximation of zero temperature gradient (isothermal flow condition) within the flow-field region may be taken (see Solinger, A., Buff, J. and Rapport, S. [45], Korobeinikov, V. P. [16], Zhuravskaya, T. A. [50]). Laumbach and Probstein (see Laumbah, D. D. and Probstein, R. F. [17]) investigated the self-similar one-dimensional flow behind a plane shock propagating upward into an exponentially decreasing atmosphere, assuming the flow to be isothermal due to large radiation mean free paths at high altitudes and significant radiative heat transfer associated with the high temperatures of an accelerating shock wave. Sachdev and Ashraf (see Sachdev, P. L. and Ashraf, S. [40]) investigated the behavior of converging spherical and cylindrical shock waves by developing self-similar solutions under the assumption of zero temperature gradient in the flow field behind the shock. The isothermal approximation can be justified in environment

where radiative cooling is highly efficient and the cooling timescale is much shorter than the dynamical timescale of the flow. Under such conditions, the post-shock gas rapidly relaxes toward a nearly constant temperature state (see Draine, B. T. [10]). Under the above assumption, the self-similar solution to the current problem for the isothermal flow case is presented in section 4. In sections 2 and 3, we have discussed the solutions for adiabatic flow case.

As known to us, in all the previous works, the self-similar solution for cylindrically symmetric shock wave in a rotating self-gravitating ideal dusty gas with the impact of magnetic field (axial or azimuthal) for isothermal and adiabatic flows has not been explored by any author, which makes this study novel from the earlier studies. To investigate a wide range of physical phenomena in astrophysics rigorously, it is necessary to address the underlying governing equations. However, obtaining exact or even numerical solutions of the system of non-linear partial differential equations is generally not feasible. Recent developments in numerical and analytical methods for partial differential equations (PDEs) have led to significant improvements in computational efficiency and accuracy. Ahmad et al. (see Ahmad, S. et al. [1]) have determined the analytical solution of the 3rd order dispersive fractional PDEs under exponential decay and Mittag-Leffer type kernels via Laplace-Adomian decomposition and found that fractional order PDEs under non-local and non-singular kernels provides better understanding than integer-order model. Shah and Akram (see Shah, K. and Akram, M. [44]) have derived the shifted Jacobi operational matrices of fractional derivatives and integration which are applied for numerical solution of general linear multi-term fractional PDEs and compared the numerical results obtained by the considered method with those found by other known methods like homotopy analysis method. Bilal et al. (see Bilal, M. et al. [3]) showed the successful implementation of the scale-3 Haar wavelets and finite difference formulation for the numerical solutions of two dimensional linear and non-linear single and coupled PDEs. From the above studies (see Ahmad, S. et al. [1], Shah, K. and Akram, M. [44] and Bilal, M. et al. [3]), we conclude that the numerical solution of the system of PDEs also play important role in the discussion of physical phenomena if closed form solutions are not possible. In our model we have used R-K 4th order technique to obtain the numerical solution of the present problem. The R-K formula for the present problem and the order of errors is presented in section 5.

From the obtained numerical solutions of the present study we conclude that the shock strength increases on increasing the gravitational parameter, or the ratio of solid-particle density to the initial gas density; whereas the shock strength decreases with an increment in the adiabatic index, or the shock Cowling number. The shock

strength is greater in the presence of an axial magnetic field as compared to that observed under an azimuthal magnetic field configuration. Moreover, the shock wave exhibits reduced strength under isothermal flow conditions in comparison to adiabatic flows.

2. Problem formulation

The influence of micrometer-sized solid particles on shock or blast wave propagation is examined under the assumption that the solid particles attain the same velocity and temperature as the surrounding ideal gas (see Pai, S. I. [31], Higashino, F. and Suzuki, T. [14], Nath, G. and Vishwakarma, J. P. [28]) $u_g = u_p = u$; $T_p = T_g = T$, where u_g is the gas's velocity, u_p is solid particle's velocity, u is the fluid velocity, T_g is the gas temperature, T_p is the solid particles temperature and T is the mixture's temperature. The mixture initially is in a non-equilibrium state, progressively approaches equilibrium through interphase momentum and heat exchange between the gas and the suspended particles (see Miura, H. and Glass, I. I. [21]). Popel et al. (see Popel, S. I. et al. [34]) have reported that an increase in the dust density results in a reduced influence of Landau damping. This agrees with experimental findings of Barkan et al. (see Barkan, A. et al. [2]), which show that the presence of negatively charged dust significantly weakens the Landau damping of dust–ion acoustic (DIA) waves, even when the ion and electron temperatures are equal. Therefore, hydrodynamic equations that incorporate nonlinear steepening effects remain applicable even in the presence of dust. The dissipative processes related to charging of dust particles that are taken into account in the hydrodynamic equations are more important than the kinetic damping (see Popel, S. I. et al. [35]). Thus, for a perfectly conducting mixture under the aforementioned conditions, the governing equations of motion become analogous to those of magnetogasdynamics flow.

The basic equations governing the one dimensional unsteady adiabatic flow of a self-gravitating rotating perfectly conducting ideal dusty gas under the impact of magnetic field are (see Nath, G. [22], Nath, G. [23], Nath, G. and Maurya, A. [24], Vishwakarma, J.P. and Nath, G. [47])

$$\begin{aligned}
&\frac{\partial \rho}{\partial t} + u\frac{\partial \rho}{\partial x} + \rho\left(\frac{\partial u}{\partial x} + \frac{u}{x}\right) = 0, \quad \frac{\partial u}{\partial t} + u\frac{\partial u}{\partial x} + \frac{1}{\rho}\frac{\partial p}{\partial x} + \frac{\mu h^2 i}{\rho x} + \frac{\mu h}{\rho}\frac{\partial h}{\partial x} + \frac{g^* m}{x} - \frac{v^2}{x} = 0,\\
&\frac{\partial h}{\partial t} + u\frac{\partial h}{\partial x} + h\frac{\partial u}{\partial x} + (1-i)\frac{uh}{x} = 0, \quad \frac{\partial U_{mix}}{\partial t} + u\frac{\partial U_{mix}}{\partial x} - \frac{p}{\rho^2}\left(\frac{\partial \rho}{\partial t} + u\frac{\partial \rho}{\partial x}\right) = 0, \qquad (3)\\
&\frac{\partial v}{\partial t} + u\left(\frac{\partial v}{\partial x} + \frac{v}{x}\right) = 0, \quad \frac{\partial w}{\partial t} + u\frac{\partial w}{\partial x} = 0, \quad \frac{\partial m}{\partial x} = 2\pi\rho x,
\end{aligned}$$

where u, w and v corresponds to the radial, axial and azimuthal fluid velocity $\vec{q}$ components, respectively in the cylindrical polar coordinates (x, θ, z); the variables

h, p and ρ denote the magnetic field, pressure, and the density of the mixture, respectively; x and t denote the spatial coordinate and time coordinate; g^* refers to the gravitational constant; m denotes the mass of the mixture contained in a unit cylinder of radius x; μ be the magnetic permeability.

For a two-phase mixture of a perfect gas and small solid particles, the corresponding equation of state can be formulated as (see Vishwakarma, J. P. and Nath, G. [47], Pai, S. I. [31])

$$p = \frac{(1-\lambda_p)}{(1-Z)}\rho R^* T, \tag{4}$$

where T denotes the temperature, R^* is the specific gas constant, ρ and p are the density and pressure of the mixture, Z is the volume fraction of solid particles and λ_p is the solid particle mass concentration in the mixture.

In the case of the pseudo-fluid corresponding to the solid particle phase, the state equation is simply expressed as $\rho_{sp} =$ constant, where ρ_{sp} corresponds to the particles species density. The relationship between λ_p and Z is $\lambda_p = \frac{\rho_{sp} Z}{\rho}$. Since the equilibrium conditions persists in the flow domain, λ_p remains constant, which implies that $\frac{Z}{\rho}$ is constant (see Vishwakarma, J. P. and Nath, G. [47], Pai, S. I. [31]). Furthermore, the following relation holds throughout the entire flow field (see Vishwakarma, J. P. and Nath, G. [47], Pai, S. I. [31])

$$Z = \frac{\lambda_p}{[\lambda_p + G(1-\lambda_p)]}, \tag{5}$$

where $G = \frac{\rho_{sp}}{\rho_g}$ is the ratio of species densities of the pseudo fluid solid particles to the gas density.

The mixture's internal energy per unit mass may be formulated as

$$U_{mix} = [C_{sp}\lambda_p + C_v(1-\lambda_p)]T = C_{vm}T, \tag{6}$$

where C_{sp} is the specific heat of the pseudo fluid of small solid particles, C_{vm} and C_v are the mixture's specific heat and gas specific heat at constant volume, respectively. For simplicity C_{sp} and C_v are assumed to be constant (see Vishwakarma, J. P. and Nath, G. [47], Pai, S. I. [31]).

The specific heat of the perfectly conducting mixture at constant pressure is expressed as

$$C_{pm} = \lambda_p C_{sp} + (1-\lambda_p)C_p, \tag{7}$$

where C_p and C_{pm} denote the specific heat of the gas and of the mixture, respectively, at constant pressure. Following the same lines as in Pai (see Pai, S. I. [31]), the ratio of specific heats for the gas-particle mixture can be expressed as follows $\Gamma = \dfrac{C_{pm}}{C_{vm}} = \dfrac{\gamma + \delta^*\epsilon^*}{1 + \delta^*\epsilon^*}$, where $\gamma = \frac{C_p}{C_v}$ denotes the ratio of the gas specific heats at constant pressure and constant volume, $\delta^* = \frac{\lambda_p}{1-\lambda_p}$, $\epsilon^* = \frac{C_{sp}}{C_v}$. Furthermore, $C_{pm} - C_{vm} = (1 - \lambda_p)R^*$, upon applying the approximation $(1 - Z) \approx 1$.

Continuing along the same reasoning as in Nath (see Nath, G. [22]), Vishwakarma and Nath (see Vishwakarma, J. P. and Nath, G. [47]), and Pai (see Pai, S. I. [31]), we can write the formula for the internal energy per unit mass, for a mixture composed of an ideal gas and a pseudo-fluid of small solid particles, as follows:

$$U_{mix} = \frac{p(1 - Z)}{(\Gamma - 1)\rho}. \tag{8}$$

At a radial distance x from the symmetry axis, the azimuthal fluid velocity (v) is directly related to the angular velocity of the medium (A^*) through the expression:

$$v = A^* x. \tag{9}$$

The vorticity vector $\vec{Y} = \frac{1}{2}\nabla \times \vec{q}$, has its components expressed as (see Levin, V. A. and Skopina, G. A. [19], Nath, G. [22]):

$$Y_x = 0, \quad Y_\theta = -\frac{1}{2}\frac{\partial w}{\partial x}, \quad Y_z = \frac{1}{2x}\frac{\partial}{\partial x}(vx). \tag{10}$$

A shock wave is assumed to be propagating outward from the axis of symmetry into the ambient medium. The medium is supposed to have constant initial density, a variable azimuthal and axial fluid velocities, zero radial velocity. The present work investigates the shock waves driven by a piston moving with time according to an exponential law (1) within a self-gravitating, rotating dusty medium under the influence of magnetic field. By invoking self-similarity, the trajectory of the shock wave is governed by relation (2). The flow variables in the pre-shock region are characterized by (see Nath, G. [22], Nath, G. and Maurya, A. [24], Vishwakarma, J. P. and Nath, G. [47]):

$$\begin{aligned} u = 0, \;\; v = v_1 = E^* \exp(jt), \;\; w = w_1 = F^* \exp(\alpha t), \\ \rho = \rho_1 = \text{constant}, \;\; h = h_1 = C^* \exp(-l_0 t), \end{aligned} \tag{11}$$

where j, E^*, F^*, C^* α, l_0 are dimensional constants, and the subscript '1' denotes the condition immediately ahead of the shock front. At a radial distance x_s, the angular velocity of the ambient medium is evaluated from Eqs. (9) and (11) as

$$A_1^* = (E^* \exp(jt))/x_{_S}. \tag{12}$$

The vorticity vector components in the region ahead of the shock front from Eq. (10) are obtained as

$$Y_{x_1} = 0, \quad Y_{\theta_1} = -\frac{F^*\alpha}{2lx_s}\exp(\alpha t), \quad Y_{z_1} = \frac{E^*(l+j)}{2lx_s}\exp(jt). \tag{13}$$

From the Eqs. (3) and (11), we get

$$m = m_1 = \pi\rho_1 x_s^2, \quad p_1 = \left(\frac{E^{*2}\rho_1}{2K_0^2} - \frac{g^*\pi\rho_1^2}{2} - \frac{\mu}{2}\frac{C^{*2}}{K_0^2}(i+1)\right)x_s^2, \qquad (j=l) \tag{14}$$

for the existence of similarity solutions, it is necessary to take $j = -l_0 = l$. From (14) it is clear that for initial pressure to be positive $\frac{E^{*2}\rho_1}{2K_0^2} > \frac{g^*\pi\rho_1^2}{2} + \frac{\mu}{2}\frac{C^{*2}}{K_0^2}(i+1)$. With the use of Eq. (5), the solid particles initial volume fraction Z_1 is obtained as

$$Z_1 = \frac{\lambda_p}{[(1-\lambda_p)G_1 + \lambda_p]}, \tag{15}$$

where $G_1 = \rho_{sp}/\rho_{g1}$ is the density ratio of the solid particles to the initial gas. The Rankine-Hugoniot jump conditions, across the cylindrical shock wave can be expressed as (see Nath, G. [22], Nath, G. and Maurya, A. [24], Vishwakarma, J. P. and Nath, G. [47])

$$\rho_2(U_s - u_2) = \rho_1 U_s, \;\; p_2 + \rho_2(U_s-u_2)^2 + \frac{\mu h_2^2}{2} = p_1 + \rho_1 U_s^2 + \frac{\mu h_1^2}{2}, \;\; \frac{Z_2}{\rho_2} = \frac{Z_1}{\rho_1},$$
$$m_2 = m_1, \;\; v_2 = v_1, w_2 = w_1, \; h_2(U_s - u_2) = h_1 U_s, \; (U_{mix})_2 + \frac{p_2}{\rho_2} + \frac{1}{2}(U_s-u_2)^2$$
$$+ \frac{\mu h_2^2}{\rho_2} = (U_{mix})_1 + \frac{p_1}{\rho_1} + \frac{1}{2}(U_s)^2 + \frac{\mu h_1^2}{\rho_1}, \tag{16}$$

where '2' corresponds to the conditions just behind the shock front. U_s $(= dx_s/dt)$ is the velocity of the shock front into the mixture. Eq. (16) can be expressed as

$$u_2 = (1-\beta)U_S, \;\; \rho_2 = \rho_1/\beta; \;\; Z_2 = \frac{Z_1}{\beta}; \;\; h_2 = \frac{h_1}{\beta}; \;\; m_2 = \pi\rho_1 x_s^2,$$
$$v_2 = E^*\, exp(jt), \;\; w_2 = F^*\, exp(\alpha t), p_2 = \rho_1 U_s^2 L, \tag{17}$$

where $L = (1-\beta) + \frac{1}{\gamma M^2} + \frac{M_A^{-2}}{2}\left(1 - \frac{1}{\beta^2}\right)$, $M = \left(\frac{U_s^2 \rho_1}{\gamma p_1}\right)^{1/2}$ is the shock-Mach number with reference to the frozen speed of sound $\left(\frac{\gamma p_1}{\rho_1}\right)^{1/2}$ in the ideal gas, and $M_A = \left(\frac{\rho_1 U_s^2}{\mu h_1^2}\right)^{1/2}$ denotes the Alfven-Mach number (inverse square root of shock Cowling number).

The density ratio denoted by β (lies between 0 and 1), across the shock front can be obtained from the following equation

$$\left(\frac{\Gamma+1}{2}\right)\beta^3 - \left(Z_1 + \frac{M_A^{-2}\Gamma}{2} + \frac{\Gamma}{\gamma M^2} + \frac{(\Gamma-1)}{2}\right)\beta^2 + \left(\frac{M_A^{-2}[\Gamma - 2 + Z_1]}{2}\right)\beta + \frac{M_A^{-2}}{2}(Z_1) = 0. \tag{18}$$

The shock jump conditions for the vorticity vector components across the shock front are (see Levin, V. A. and Skopina, G. A. [19], Nath, G. [22])

$$Y_{\theta_2} = Y_{\theta_1}/\beta, \qquad Y_{z_2} = Y_{z_1}/\beta. \tag{19}$$

For the existence of similarity solution, M and M_A should be constants, thus, we have $j = -l_0 = l$. The relationship between M and M_A^{-2} is obtained as follows $M^2 = \frac{2}{\gamma[R_0 - g_0^* - M_A^{-2}(1+i)]}$, where $R_0 = \frac{E^{*2}}{K_0^2 l^2}$ is the rotational parameter and $g_0^* = \frac{g^* \pi \rho_1}{l^2}$ is taken as the gravitational parameter, and M_A^{-2} is the shock Cowling number. It follows from this relation that for $R_0 = 0$ with $g_0^* \neq 0$, $M_A^{-2} \neq 0$ or $g_0^* = 0$, $M_A^{-2} \neq 0$ or $g_0^* \neq 0$, $M_A^{-2} = 0$ the shock Mach number M takes the imaginary values, and hence the problem can not reduce to non-rotating medium case. However for non-rotating, non-gravitating and non-magnetic case (i.e., for $R_0 = 0$, $g_0^* = 0$, $M_A^{-2} = 0$), the shock Mach number becomes infinite (i.e., $M = \infty$) which corresponds to strong shock (i.e., $p_1 \approx 0$) in this case our problem reduces to Vishwakarma and Nath (see Vishwakarma, J. P. and Nath, G. [47]) problem for non-gravitating and non-rotating without magnetic field.

3. Similarity transformation and solution

In order to derive the similarity solutions, the physical variables may be represented by (see Nath, G. [22], Rao, M. P. R. and Ramana, B. V. [37], Vishwakarma, J. P. and Nath, G. [47])

$$u = U_S W(\eta), \quad v = U_s V(\eta), \quad w = U_s \psi(\eta), \quad \rho = \rho_1 D(\eta), \quad Z = Z_1 D(\eta),$$
$$m = m_1 \phi(\eta), \quad p = \rho_1 U_S^2 P(\eta), \sqrt{\mu} h = \rho_1^{1/2} U_s B(\eta), \tag{20}$$

where the quantities P, B, W, V, ψ, D and ϕ are the functions of the non-dimensional similarity variable $\eta = x/x_s$. The similarity variable η attains the value unity at the shock front and η_p at the inner boundary (or the piston surface). Using Eqs. (1), (2), and (20), the relationship between I_0 and K_0 can be obtained in the following form:

$$I_0 = \eta_p K_0. \tag{21}$$

By employing the transformations (20), the governing equations (3) are transformed into a system of ordinary differential equations (ODEs) as given below

$$\begin{aligned}
&\frac{dD}{d\eta} = -\frac{D}{(W-\eta)}\left[\frac{dW}{d\eta} + \frac{W}{\eta}\right], \quad \frac{dB}{d\eta} = \frac{-B}{(W-\eta)}\left[\frac{\eta + (1-i)W}{\eta} + \frac{dW}{d\eta}\right], \\
&\frac{dV}{d\eta} = \frac{-V}{(W-\eta)}\frac{(W+\eta)}{\eta}, \quad \frac{d\psi}{d\eta} = \frac{-\psi}{(W-\eta)}, \quad \frac{d\phi}{d\eta} = 2\eta D, \\
&\frac{dP}{d\eta} = -D\left(W + \frac{g_0^*\phi}{\eta} - \frac{V^2}{\eta}\right) + \left(\frac{B^2 - D(W-\eta)^2}{(W-\eta)}\right)\frac{dW}{d\eta} \\
&+ \frac{B^2}{(W-\eta)\eta}[\eta(1+i) + W(1-2i)], \\
&\frac{dW}{d\eta} = \frac{-2P\eta + D(W-\eta)[W\eta + g_0^*\phi - V^2] - B^2[\eta(i+1) + W(1-2i)] - DW\Delta}{\eta(D\Delta + B^2 - D(W-\eta)^2)},
\end{aligned} \tag{22}$$

where $\Delta = \frac{P\Gamma}{D(1-Z_1 D)}$.

The adiabatic compressibility is obtained by the following formula

$$\tau_{adi} = \frac{1}{\rho a_{adi}^2} = \frac{1}{\rho}\left(\frac{\partial \rho}{\partial p}\right)_S = \frac{(1-Z)}{\Gamma p}, \tag{23}$$

where a_{adi} is the adiabatic speed of sound in the mixture, expressed as $a_{adi}^2 = \frac{\Gamma p}{\rho(1-Z)}$.

By using Eqs. (20) and (23), we get the non-dimensional adiabatic compressibility τ_{adi} expression as

$$\rho_1 U_s^2 \tau_{adi} = \frac{(1 - Z_1 D)}{\Gamma P}. \tag{24}$$

With the aid of similarity transformations given in Eq. (20), the jump conditions (17) can be written as

$$\begin{aligned}
&W(1) = (1-\beta); \quad V(1) = \frac{E^*}{K_0 l}; \quad \psi(1) = \frac{F^*}{K_0 l}; \quad D(1) = \frac{1}{\beta}; \quad \phi(1) = 1; \\
&P(1) = L; \quad B(1) = \frac{M_A^{-1}}{\beta},
\end{aligned} \tag{25}$$

where it is necessary to take $\alpha = j = l$ to get the similarity solutions. At the piston surface, the fluid must satisfy the kinematic boundary condition. Mathematically, it is written as

$$W(\eta_p) = \eta_p. \tag{26}$$

With the use of similarity transformations (20) in Eq. (10), the vorticity vector components in the non-dimensional form $\Pi_x = Y_x/(U_s/x_s)$, $\Pi_\theta = Y_\theta/(U_s/x_s)$, $\Pi_z = Y_z/(U_s/x_s)$ are derived as

$$\Pi_x = 0, \quad \Pi_\theta = \frac{\psi}{2(W-\eta)}, \quad \Pi_z = \frac{-V}{(W-\eta)}. \tag{27}$$

4. Isothermal Flow

In the present section, we have discussed the similarity solution corresponding to isothermal flow. In extremely high-temperature flows, such as those generated right after a strong explosion, the heat flux becomes so intense that the temperature distribution remains nearly uniform. Consequently, the temperature gradient tends to vanish, i.e., $\partial T/\partial x \to 0$ and $T = T(t)$, and such flows are classified as isothermal flow. The isothermal behavior of the flow behind a strong shock has been shown from the approximate solution to the radiating point explosion problem in an exponential atmosphere obtained by Laumbach and Probstein (see Laumbach, D.D. and Probstein, R. F. [18]). The corresponding case in which radiation is not considered and the flow behind the shock is taken to be adiabatic has been considered by Raizer (see Raizer, Y. P. [36]), Grover and Hardy (see Grover, R. and Hardy, J. W. [12]). For the isothermal flow, the fundamental equations (3) will be same except the radial momentum conservation equation and the energy equation. These two equations will be replaced by (see Korobeinikov, V. P. [16], Zhuravskaya, T. A. and Levin, V. A. [50], Laumbach, D. D. and Probstein, R. F. [17])

$$\frac{\partial u}{\partial t} + u\frac{\partial u}{\partial x} + \frac{(1-\lambda_p)R^*T}{\rho(1-Z)^2}\frac{\partial \rho}{\partial x} + \frac{g^*m}{x} - \frac{v^2}{x} + \frac{1}{\rho}\left(\frac{\mu h^2 i}{x} + \mu h\frac{\partial h}{\partial x}\right) = 0, \quad \frac{\partial T}{\partial x} = 0, \tag{28}$$

where $\left(\frac{\partial p}{\partial \rho}\right)_T = \frac{p}{\rho(1-Z)}$ expresses the square of isothermal sound speed, a^2_{iso} in the mixture.

The emergence of an isothermal shock follows from a mathematical approximation in which the heat flux is taken to be proportional to the temperature gradient,

thereby ruling out the occurrence of a temperature discontinuity across the shock hence the Rankine-Hugoniot jump conditions (16) for isothermal flow becomes (see Zel'dovich, Y. B. and Raizer, Y. P. [49], Rosenau, P. and Frankenthal, S. [38], Rosenau, P. and Frankenthal, S. [39]):

$$\rho_2(U_s-u_2)=\rho_1 U_s,\;\; p_2+\rho_2(U_s-u_2)^2+\frac{\mu h_2^2}{2}=p_1+\rho_1 U_s^2+\frac{\mu h_1^2}{2},\;\; \frac{Z_2}{\rho_2}=\frac{Z_1}{\rho_1},$$
$$m_2=m_1,\;\; v_2=v_1, w_2=w_1,\;\; h_2(U_s-u_2)=h_1 U_s,\;\; (U_{mix})_2+\frac{p_2}{\rho_2}+\frac{1}{2}(U_s-u_2)^2$$
$$+\frac{\mu h_2^2}{\rho_2}+\frac{q_2}{\rho_1 U_s}=(U_{mix})_1+\frac{p_1}{\rho_1}+\frac{1}{2}(U_s)^2+\frac{\mu h_1^2}{\rho_1}+\frac{q_1}{\rho_1 U_s}. \tag{29}$$

Since the shock is strong one having finite Mach number, the term (q_2-q_1) is assumed to be negligible as compared with the product p_2U_s (see Nath, G. [22], Vishwakarma, J. P. [47], Laumbach, D.D. and Probstein, R. F. [17]). Under this approximation, the resulting expression for β and the R-H jump conditions together with kinematic condition will be same as given by Eqs. (18), (25) and (26), respectively.

Using Eqs. (4) and (28), we get

$$\frac{p}{p_2}=\frac{(1-Z_2)\rho}{(1-Z)\rho_2}. \tag{30}$$

Eqs. (17), (20) and (30) are used to obtain the relationship between P and D as

$$P(\eta)=L\left[\frac{D(\beta-Z_1)}{(1-Z_1D)}\right]. \tag{31}$$

Through the application of the similarity transformations (20), Eqs. (3), (28) can be reformulated and simplified to

$$\frac{dD}{d\eta}=-\frac{D}{(W-\eta)}\left[\frac{dW}{d\eta}+\frac{W}{\eta}\right],\quad \frac{dB}{d\eta}=\frac{-B}{(W-\eta)}\left[\frac{\eta+(1-i)W}{\eta}+\frac{dW}{d\eta}\right],$$
$$\frac{dV}{d\eta}=\frac{-V}{(W-\eta)}\frac{(W+\eta)}{\eta},\quad \frac{d\psi}{d\eta}=\frac{-\psi}{(W-\eta)},\quad \frac{d\phi}{d\eta}=2\eta D, \tag{32}$$
$$\frac{dW}{d\eta}=\frac{-D(W-\eta)[W\eta+g_0^*\phi-V^2]-B^2[i(W-\eta)-(\eta+(1-i)W)]+DW\Lambda}{\eta[D(W-\eta)^2-B^2-D\Lambda]},$$

where $\Lambda=\frac{P}{D[(1-Z_1D)]}$.

The isothermal compressibility (τ_{iso}), is obtained from

$$\tau_{iso}=\frac{1}{\rho a_{iso}^2}=\frac{(1-Z)}{p}. \tag{33}$$

Eqs. (20) and (33) yields the non-dimensional isothermal compressibility's expression as follows

$$\rho_1 U_s^2 \tau_{iso} = \frac{(1 - Z_1 D)}{P}. \tag{34}$$

After the normalization of the flow variables v, w, u, ρ, m, p and h, we obtain

$$\begin{gathered} \frac{v}{v_2} = \frac{V(\eta)}{V(1)}, \ \frac{w}{w_2} = \frac{\psi(\eta)}{\psi(1)}, \ \frac{u}{u_2} = \frac{W(\eta)}{W(1)}, \ \frac{\rho}{\rho_2} = \frac{D(\eta)}{D(1)}, \\ \frac{m}{m_2} = \frac{\phi(\eta)}{\phi(1)}, \ \frac{p}{p_2} = \frac{P(\eta)}{P(1)}, \ \frac{h}{h_2} = \frac{B(\eta)}{B(1)}. \end{gathered} \tag{35}$$

5. Numerical method and order of errors

To determine the distribution of physical flow variables, numerical integration is carried out for the system of ODEs (22) and Eqs (24) and (27) for the case of adiabatic flow, and the set of ODEs (32) and Eqs. (31) and (34) for the case of isothermal flow along with the boundary conditions (25) and (26) by using fourth-order Runge–Kutta method via Mathematica software. The number of steps is taken to be one thousand by default. Thus, the value of the step size ϵ is equal to the distance between a neighboring point to the piston surface and the shock wave front divided by one thousand, see for example, for adiabatic case for curve 1 in Fig. 2, $\epsilon = 4.0062 \times 10^{-5}$. The Runge-Kutta method of order four gives the interpolating function value correct to the first four powers of ϵ and has, therefore, errors of the order of ϵ^5. For the adiabatic flow case, the Runge-Kutta fourth-order formulae for set of Eqs. (22) are obtained as (see Vishwakarma, J. P. and Nath, G. [48], Nath, G. and Maurya, A. [29])

$$D(\eta + \epsilon) = D(\eta) + \frac{1}{6}(\mathcal{K}_{01} + 2\mathcal{K}_{11} + 2\mathcal{K}_{21} + \mathcal{K}_{31}) + \mathcal{O}(\epsilon^5), \tag{36}$$

$$B(\eta + \epsilon) = B(\eta) + \frac{1}{6}(\mathcal{K}_{02} + 2\mathcal{K}_{12} + 2\mathcal{K}_{22} + \mathcal{K}_{32}) + \mathcal{O}(\epsilon^5), \tag{37}$$

$$V(\eta + \epsilon) = V(\eta) + \frac{1}{6}(\mathcal{K}_{03} + 2\mathcal{K}_{13} + 2\mathcal{K}_{23} + \mathcal{K}_{33}) + \mathcal{O}(\epsilon^5), \tag{38}$$

$$\psi(\eta + \epsilon) = \psi(\eta) + \frac{1}{6}(\mathcal{K}_{04} + 2\mathcal{K}_{14} + 2\mathcal{K}_{24} + \mathcal{K}_{34}) + \mathcal{O}(\epsilon^5), \tag{39}$$

$$\phi(\eta+\epsilon)=\phi(\eta)+\frac{1}{6}(\mathcal{K}_{05}+2\mathcal{K}_{15}+2\mathcal{K}_{25}+\mathcal{K}_{35})+\mathcal{O}(\epsilon^5), \tag{40}$$

$$P(\eta+\epsilon)=P(\eta)+\frac{1}{6}(\mathcal{K}_{06}+2\mathcal{K}_{16}+2\mathcal{K}_{26}+\mathcal{K}_{36})+\mathcal{O}(\epsilon^5), \tag{41}$$

$$W(\eta+\epsilon)=W(\eta)+\frac{1}{6}(\mathcal{K}_{07}+2\mathcal{K}_{17}+2\mathcal{K}_{27}+\mathcal{K}_{37})+\mathcal{O}(\epsilon^5), \tag{42}$$

with

$$\mathcal{K}_{0\sigma}=\epsilon f_\sigma(\eta,D(\eta),B(\eta),V(\eta),\psi(\eta),\phi(\eta),P(\eta),W(\eta)), \tag{43}$$

$$\mathcal{K}_{1\sigma}=\epsilon f_\sigma\left(\eta+\frac{\epsilon}{2},D(\eta)+\frac{\mathcal{K}_{01}}{2},B(\eta)+\frac{\mathcal{K}_{02}}{2},V(\eta)+\frac{\mathcal{K}_{03}}{2},\psi(\eta)+\frac{\mathcal{K}_{04}}{2},\phi(\eta)+\frac{\mathcal{K}_{05}}{2},P(\eta)+\frac{\mathcal{K}_{06}}{2},W(\eta)+\frac{\mathcal{K}_{07}}{2}\right), \tag{44}$$

$$\mathcal{K}_{2\sigma}=\epsilon f_\sigma\left(\eta+\frac{\epsilon}{2},D(\eta)+\frac{\mathcal{K}_{11}}{2},B(\eta)+\frac{\mathcal{K}_{12}}{2},V(\eta)+\frac{\mathcal{K}_{13}}{2},\psi(\eta)+\frac{\mathcal{K}_{14}}{2},\phi(\eta)+\frac{\mathcal{K}_{15}}{2},P(\eta)+\frac{\mathcal{K}_{16}}{2},W(\eta)+\frac{\mathcal{K}_{17}}{2}\right), \tag{45}$$

$$\mathcal{K}_{3\sigma}=\epsilon f_\sigma(\eta+\epsilon,D(\eta)+\mathcal{K}_{21},B(\eta)+\mathcal{K}_{22},V(\eta)+\mathcal{K}_{23},\psi(\eta)+\mathcal{K}_{24},\phi(\eta)+\mathcal{K}_{25},P(\eta)+\mathcal{K}_{26},W(\eta)+\mathcal{K}_{27}), \tag{46}$$

where $\sigma = 1,\ 2,\ 3,\ 4$; and the higher order terms $\mathcal{O}(\epsilon^5)$, are neglected during the numerical calculations. In a similar manner, the fourth-order Runge–Kutta formulae for set of Eqs. (32) can be obtained for the isothermal flow case.

6. Results and discussion

For this computational work, the values of the problem physical parameters used are taken as (see Pai, S. I. et al. [30], Vishwakarma, J. P. and Nath, G. [47], Nath, G. [26], Nath, G. [27], Miura, H. and Glass, I. I. [21]): $\lambda_p = 0, 0.1, 0.2$; $\gamma = 4/3, 7/5$; $M_A^{-2} = 0, 0.02, 0.04$; $G_1 = 5, 20, 100$ $g_0^* = 0, 0.05, 3, 6$; $R_0 = 0, 0.1$; $M = 5$. The results obtained are presented graphically in Figs. 1 and 2 are summarized numerically in Tables 1 and 2.

In the limiting case of non-rotating, non-gravitating and non-magnetic (i.e., for $R_0 = 0, g_0^* = 0, M_A^{-2} = 0$), the set of Eqs. (22) for adiabatic flow, and Eqs. (31) and (32) for isothermal flow, reduces to Eqs. (31)-(33) for adiabatic case, and Eqs. (24)-(26) for isothermal case, respectively, and the jump conditions (25) to jump

conditions (27) of Vishwakarma and Nath (see Vishwakarma, J. P. and Nath, G. [47]). Vishwakarma and Nath (see Vishwakarma, J. P. and Nath, G. [47]) have performed the numerical calculations for spherical symmetry, but in the present problem, we have considered the cylindrical case for numerical computation. It is found that for cylindrical geometry in non-rotating, non-gravitating and non-magnetic case (i.e., for $R_0 = 0, g_0^* = 0, M_A^{-2} = 0$) the shock strength increases on increasing G_1 at constant λ_p, but the shock strength decreases on increasing λ_P for smaller value of G_1, which are consistent with the results obtained by Vishwakarma and Nath (see Vishwakarma, J. P. and Nath, G. [47]) for spherical geometry (see Table 1). The curves corresponding to Vishwakarma and Nath (see Vishwakarma, J. P. and Nath, G. [47]) work are shown as curves 1 to 3 in Figures 1 and 2, and the computed values are presented in Tables 1 and 2. Moreover, for non-rotating, non-gravitating, and non-magnetic case, the flow variables ρ/ρ_2, p/p_2 and u/u_2 decrease with increase in λ_p, but these variables increase with increase in G_1. This result is also in good agreement with the result obtained by Vishwakarma and Nath (see Vishwakarma, J.P. and Nath, G. [47]) for spherical geometry (see in curves 1, 2, 3 Fig. 1 (a, f, g)).

6.1. The effect of an increment in γ

With an increment in γ, the shock wave decay (see Table 1), i.e., the distance between the piston and shock front increases. The flow variables v/v_2, u/u_2, w/w_2, Π_θ and m/m_2 increase with γ; whereas ρ/ρ_2 and Π_z decrease on increasing γ (see Figs. 1(a, c - e, g - i)). Also, the compressibility increases near the location of the piston, and it decreases near the location of the shock front (see Fig. 1(j)). The magnetic field h/h_2 increases for isothermal flow; whereas it increases near the location of piston and decreases near the location of shock front for the adiabatic flow (see Fig. 1(b)). For the isothermal case, the fluid pressure p/p_2 decreases, but for the adiabatic flow case, it decreases near the piston position and increases near the position of the shock front (see Fig. 1(f)). It is important to notice that the above effects of γ on the flow variables and on the shock is new one.

6.2.The effect of an increment in λ_p

The flow variables v/v_2, w/w_2, m/m_2, Π_θ increase, but u/u_2, ρ/ρ_2 and Π_z decrease on increasing λ_p (see Fig. 1(a, c−e, g−i)). The magnetic field h/h_2 increases near the location of the piston, and it decreases near the location of the shock front on increasing λ_p (see Fig. 1(b)). For the isothermal flow case the pressure p/p_2 decreases, but it increases for adiabatic flow with an increase in λ_p. In the absence of rotation, gravitation and magnetic field the pressure p/p_2 decreases for both adiabatic and isothermal flows with increasing λ_p (see Fig. 1(f)). The isothermal compressibility decreases, but adiabatic compressibility increases near

Table 1: The density ratio β ($= \rho_1/\rho_2$) across the shock wave front and the piston surface position η_p for different values of R_0 (rotational parameter), g_0^* (gravitational parameter), M_A^{-2} (shock Cowling number), γ (adiabatic index), λ_p (mass concentration of the solid particles), and G_1 (ratio of species densities of the solid particles to the initial gas density) with axial magnetic field ($i = 0$) or without magnetic field ($M_A^{-2} = 0$)

i	R_0	g_0^*	M_A^{-2}	M	γ	λ_p	Γ	G_1	Z_1	β	$\eta_p(adiabatic)$	$\eta_p(isothermal)$	
-	0	0	0	∞	4/3	0	1.33	-	-	0.142857	0.964485	0.942 893	Ref. Vishwakarma, J.P. and Nath, G. [47]
						0.1	1.3	5	0.0217391	0.149338	0.957056	0.937 613	
								20	0.00552486	0.135239	0.965290	0.945 193	
								100	0.00110988	0.1314	0.967432	0.947 245	
						0.2	1.2667	5	0.047619	0.159664	0.948198	0.930 247	
								20	0.0123457	0.12854	0.965488	0.947 007	
								100	0.00249377	0.119847	0.97026	0.951 633	
					7/5	0	1.4	-	-	0.166667	0.957586	0.933 641	
						0.1	1.36	5	0.0217391	0.170965	0.95129	0.929 099	
								20	0.00552486	0.157224	0.959077	0.936 581	
								100	0.00110988	0.153483	0.961186	0.938 608	
						0.2	1.32	5	0.047619	0.178982	0.939961	0.922 533	
								20	0.0123457	0.148574	0.959938	0.939 096	
								100	0.00249377	0.140081	0.964679	0.943 166	
0	0.1	0.05	0.02	7.07107	4/3	0	1.33	-	-	0.200000	0.945505	0.927984	
						0.1	1.3	5	0.0217391	0.202149	0.942254	0.924276	
								20	0.00552486	0.193435	0.946732	0.930008	
								100	0.00110988	0.191184	0.947733	0.931478	
						0.2	1.2667	5	0.047619	0.207027	0.936221	0.918536	
								20	0.0123457	0.187336	0.947626	0.931699	
								100	0.00249377	0.182469	0.949868	0.934932	
				6.90060	7/5	0	1.4	-	-	0.218696	0.940378	0.920385	
						0.1	1.36	5	0.0217391	0.219803	0.937127	0.916988	
								20	0.00552486	0.210522	0.942064	0.922980	
								100	0.00110988	0.208098	0.943210	0.924536	
						0.2	1.32	5	0.047619	0.223600	0.931275	0.911641	
								20	0.0123457	0.202814	0.943387	0.925252	
								100	0.00249377	0.197544	0.945930	0.928685	

the location of the piston, and it decreases near the location of the shock front (see Fig. (j)). The density ratio β at the shock front increases for $G_1 = 5$; whereas it decreases for $G_1 = 20$ or 100 on increasing λ_p, resulting in a decrease in the shock strength for smaller values of G_1, and an increase in the shock strength for larger values of G_1 (see Table 2). It is important to note that the results presented above are in excellent agreement with earlier results of Vishwakarma and Nath (see Vishwakarma, J.P. and Nath, G. [47]) for non-gravitating, non-rotating ideal dusty gas in absence of magnetic field.

6.3. The effect of change in G_1

The flow variables m/m_2, Π_θ, v/v_2, w/w_2 and density ratio β at the shock front

Table 2: The density ratio β $(= \rho_1/\rho_2)$ across the shock wave front and the piston surface position η_p for different values of M (shock mach number), M_A^{-2} (shock Cowling number), g_0^* (gravitational parameter), and R_0 (rotational parameter) for $\gamma = 1.4$, $\Gamma = 1.32$, $Z_1 = 0.0123457$, $\lambda_p = 0.2$, and $G_1 = 20$ with magnetic field-axial $(i = 0)$ or azimuthal $(i = 1)$ or without magnetic field $(M_A^{-2} = 0)$

M	M_A^{-2}	i	g_0^*	R_0	β	$\eta_p(adiabatic)$	$\eta_p(isothermal)$	
∞	0	-	0	0	0.148574	0.959938	0.939100	(Ref. Vishwakarma, J.P.
5	0	-	0	0.0571429	0.181086	0.951736	0.925352	and Nath, G. [47])
			3	3.05714		0.953633	0.931275	
			6	6.05714		0.955223	0.935868	
	0.02	0	0	0.0771429	0.216754	0.939843	0.918815	
			3	3.07714		0.942182	0.924341	
			6	6.07714		0.944147	0.928666	
		1	0	0.0971429		0.928932	0.909740	
			3	3.09714		0.931952	0.915586	
			6	6.09714		0.934479	0.920207	
	0.04	0	0	0.0971429	0.246966	0.929852	0.912002	
			3	3.09714		0.932589	0.917406	
			6	6.09714		0.934864	0.921671	
		1	0	0.1371429		0.913286	0.897128	
			3	3.313714		0.916984	0.903166	
			6	6.13714		0.920073	0.907992	

decrease, but ρ/ρ_2, u/u_2, Π_z, compressibility and the shock strength increase on increasing G_1 (see Figs. 1(a, c-e, g-j) and Table 1). The flow variable h/h_2 decreases near the position of the piston, and it increases near the location of the shock front (see Fig. 1(b)). The pressure p/p_2 increases for isothermal flow, but it decreases for adiabatic flow on increasing G_1 (see Fig. 1(f)). In the absence of rotation, gravitation and magnetic field the pressure p/p_2 and isothermal compressibility increase but the adiabatic compressibility decreases near the piston surface and increases near the shock front (see Fig. 1(f, j)).

Physically, at fixed value of λ_p, an increase in G_1 significantly lowers the volume fraction of small solid particles Z_1 in the mixture making Z_1 comparatively very small. Consequently, greater compression of the perfectly conducting mixture behind the shock front occur, which results in the aforementioned effects on the shock wave and flow variables. The above obtained results show that the effect of G_1 on shock wave in the present problem is similar to the results of Vishwakarma and Nath (see Vishwakarma, J. P. and Nath, G. [47]).

6.4. The effect of gravitational parameter g_0^*

The flow variables ρ/ρ_2, h/h_2, u/u_2, Π_z and the shock strength increase; whereas v/v_2, w/w_2, m/m_2 and Π_θ decrease on increasing the g_0^* (see Figs. 2(a-e, g, h, i)).

In the case of isothermal flow p/p_2 increases, but for adiabatic flow, it increases near the location of shock front and decreases near the location of the piston (see Fig. 2(f)). The isothermal compressibility decreases, but the adiabatic compressibility increases near the piston position and decreases near the shock front position with g_0^* (see Fig. 2(j)). In view of Table 2 and Figs. 2(a)–2(j), it is evident that the parameters R_0 and g_0^* influence the physical flow variables in a similar manner at constant shock Mach number $M = 5$. Both parameters produce similar effects on the distance between the shock wave front and the piston surface, as well as on the strength of the shock wave.

It is significant to note that the effects of gravitational parameter g_0^* in rotating medium is new one as this is not deliberated earlier by any one for exponential shock wave in self-gravitating rotating ideal dusty gas in presence of magnetic field.

6.5. The effect of an increment in shock Cowling number M_A^{-2}

The variables v/v_2, w/w_2, m/m_2, Π_θ, density ratio at the shock front and compressibility increase; whereas ρ/ρ_2, h/h_2, Π_z and shock strength decrease on increasing M_A^{-2} (see Figs. 2(a-e, h, i, j) and Table 2). For adiabatic flow the pressure p/p_2 and radial fluid velocity u/u_2 increase near piston surface, and these decrease near shock front on increasing magnetic field strength; whereas p/p_2 decreases and u/u_2 increases in case of isothermal flow (see Figs. 2(f, g)). The disturbed region between the shock and piston widens as M_A^{-2} increases, and hence the magnetic flux is less compressed, which results in the decrease in the magnetic field h/h_2.

It should be noted that the effects of magnetic field on the physical variables and on shock strength presented above is new one as this is not deliberated earlier by any one for exponential shock wave in self-gravitating rotating ideal dusty gas in presence of magnetic field.

6.6. The influence of changing the magnetic field from axial ($i = 0$) to azimuthal ($i = 1$)

The flow variables h/h_2, m/m_2, Π_θ, v/v_2, w/w_2 and compressibility increase, but the shock strength, ρ/ρ_2, p/p_2, u/u_2 and Π_z decrease due to change in magnetic field from axial to azimuthal (Figs. 2(a-j) and Table 2). This can be explained as when the magnetic field is axial the magnetic field lines are parallel to the axis of cylinder and normal to the shock front; whereas in case of an azimuthal magnetic field the lines of magnetic fields are tangential to the surface of cylinder. Shock wave is generally stronger in the presence of axial magnetic field as compared to the azimuthal magnetic field, this difference arises because azimuthal magnetic fields create higher magnetic pressure and tension, which exert a stronger resisting force on the propagating shock wave, thus lowering its strength; whereas an axial field provides less resistance.

7. Limitations

The present study has following limitations:

- The analysis is restricted to self-similar solutions, which limits its applicability to flows that strictly satisfy similarity conditions. Real physical systems often deviate from self-similar behavior, leading to the emergence of non-self-similar solutions. In the present problem similarity solution exist only if the initial density of the medium is constant.
- The collisions between solid particles of different size are not considered. In realistic dusty flows, collisions between particles of different sizes can lead to momentum and energy exchange and deviation from equilibrium with the gas, but the consideration of micro-size solid particles and dust charging results in equilibrium.
- Due to the consideration of self-gravitating gas and the presence of magnetic field impose restrictions such that $j = -l_0 = l$, and $\frac{E^{*2}\rho_1}{2K_0^2} > \frac{g^*\pi\rho_1^2}{2} + \frac{\mu}{2}\frac{C^{*2}}{K_0^2}(i+1)$ for initial pressure p_1 to be positive and Mach number to be real constant.

8. Conclusion

In the current work, the propagation of cylindrically symmetric shock waves in a self-gravitating ideal dusty gas under the influence of rotational effect of the medium with axial or azimuthal magnetic fields is examined. On the basis of the present work, we may conclude the following:

- The shock front distance from the piston is smaller for adiabatic flow case as compared with the isothermal flow, which reflects that the shock wave is more powerful in adiabatic flow rather than in the case of isothermal flow.
- Shock wave strength enhances with an increment in solid particle mass concentration (λ_p) when $G_1 \geq 20$, but for $G_1 = 5$, the shock strength decreases with increment in λ_p.
- On increasing γ or M_A^{-2} or on changing the magnetic field from axial ($i = 0$) to azimuthal ($i = 1$) the shock strength decreases.
- The shock strength increases due to the consideration of self-gravitating gas or rotating medium or by increasing the ratio of species densities of the solid particles to the gas initial density G_1.

The results of this study may be relevant for the analysis of spacecraft measurement data in the solar wind and near-Earth environment, as well as for experimental investigations involving exploding wires and cylindrically symmetric hyperbolic flows associated with re-entry vehicles or meteoric phenomena (see Nath, G. [26], Nath, G. [27]).

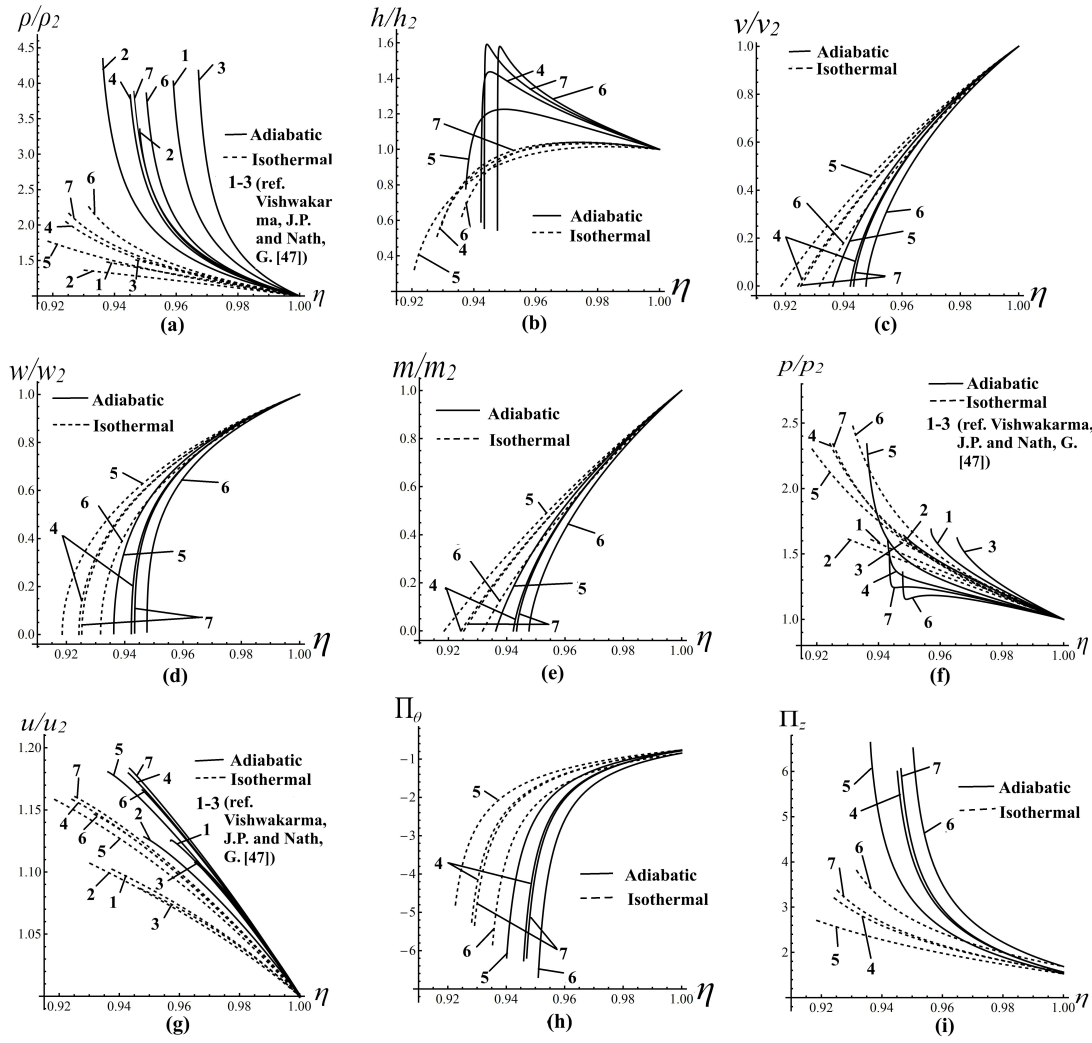

Fig. 1. The flow variables distribution in the region behind the shock front with different values of M_A^{-2}, R_0, g_0^*, γ, λ_p, G_1. (a) density ρ/ρ_2, (b) magnetic field h/h_2, (c) azimuthal velocity v/v_2, (d) axial velocity w/w_2, (e) mass m/m_2, (f) pressure p/p_2, (g) radial velocity u/u_2, (h) azimuthal vorticity vector Π_θ, (i) axial vorticity vector Π_z, (j) compressibility; $1.M_A^{-2} = 0$, $R_0 = 0$, $g_0^* = 0$, $\gamma = 4/3$, $\lambda_p = 0.1$, $G_1 = 5$ (Vishwakarma, J.P. and Nath, G. [47]); $2.M_A^{-2} = 0$, $R_0 = 0$, $g_0^* = 0$, $\gamma = 4/3$, $\lambda_p = 0.2$, $G_1 = 5$ (Vishwakarma, J.P. and Nath, G. [47]); $3.M_A^{-2} = 0$, $R_0 = 0$, $g_0^* = 0$, $\gamma = 4/3$, $\lambda_p = 0.2$, $G_1 = 20$ (Vishwakarma, J.P. and Nath, G. [47]); $4.M_A^{-2} = 0.2$, $i = 0$, $R_0 = 0.1$, $g_0^* = 0.05$, $\gamma = 4/3$, $\lambda_p = 0.1$, $G_1 = 5$; 5. $M_A^{-2} = 0.2$, $i = 0$, $R_0 = 0.1$, $g_0^* = 0.05$, $\gamma = 4/3$, $\lambda_p = 0.2$, $G_1 = 5$; 6. $M_A^{-2} = 0.2$, $i = 0$, $R_0 = 0.1$, $g_0^* = 0.05$, $\gamma = 4/3$, $\lambda_p = 0.2$, $G_1 = 20$; 7. $M_A^{-2} = 0.2$, $i = 0$, $R_0 = 0.1$, $g_0^* = 0.05$, $\gamma = 7/5$, $\lambda_p = 0.2$, $G_1 = 20$.

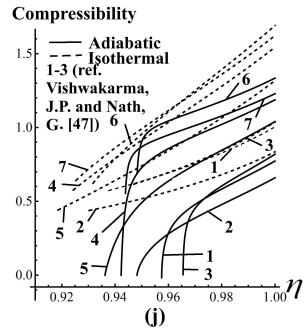

Fig. 1. Continued.

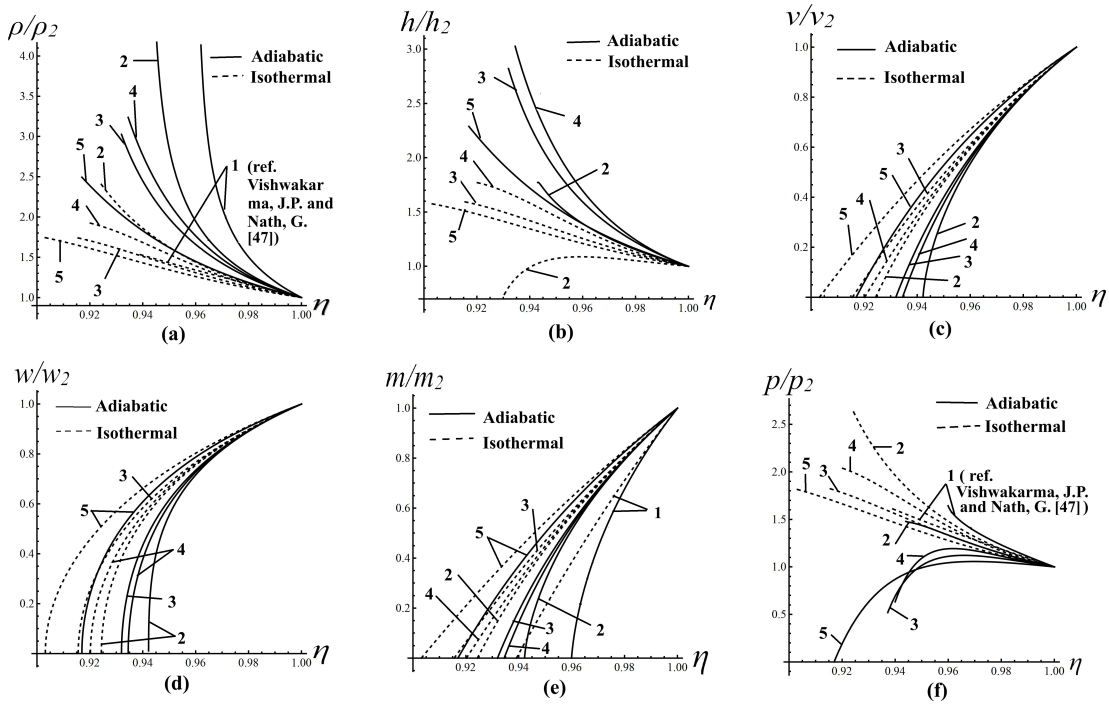

Fig. 2. The flow variables distribution in the region behind the shock front with different values of M_A^{-2}, M and g_0^* for axial ($i = 0$) and azimuthal ($i = 1$) magnetic field with $\lambda_P = 0.2$, $G_1 = 20$, $\gamma = 1.4$. (a) density ρ/ρ_2, (b) magnetic field h/h_2, (c) azimuthal velocity v/v_2, (d) axial velocity w/w_2, (e) mass m/m_2, (f) pressure p/p_2, (g) radial velocity u/u_2, (h) azimuthal vorticity vector Π_θ, (i) axial vorticity vector Π_z, (j) compressibility; 1. $M_A^{-2} = 0$, $g_0^* = 0$, $M = \infty$ (Vishwakarma, J.P. and Nath, G. [47]); 2.$M_A^{-2} = 0.02$, $g_0^* = 3$, $i = 0$, $M = 5$; 3.$M_A^{-2} = 0.02$, $g_0^* = 3$, $i = 1$, $M = 5$; 4.$M_A^{-2} = 0.02$, $g_0^* = 6$, $i = 1$, $M = 5$; 5. $M_A^{-2} = 0.04$, $g_0^* = 3$, $i = 1$, $M = 5$.

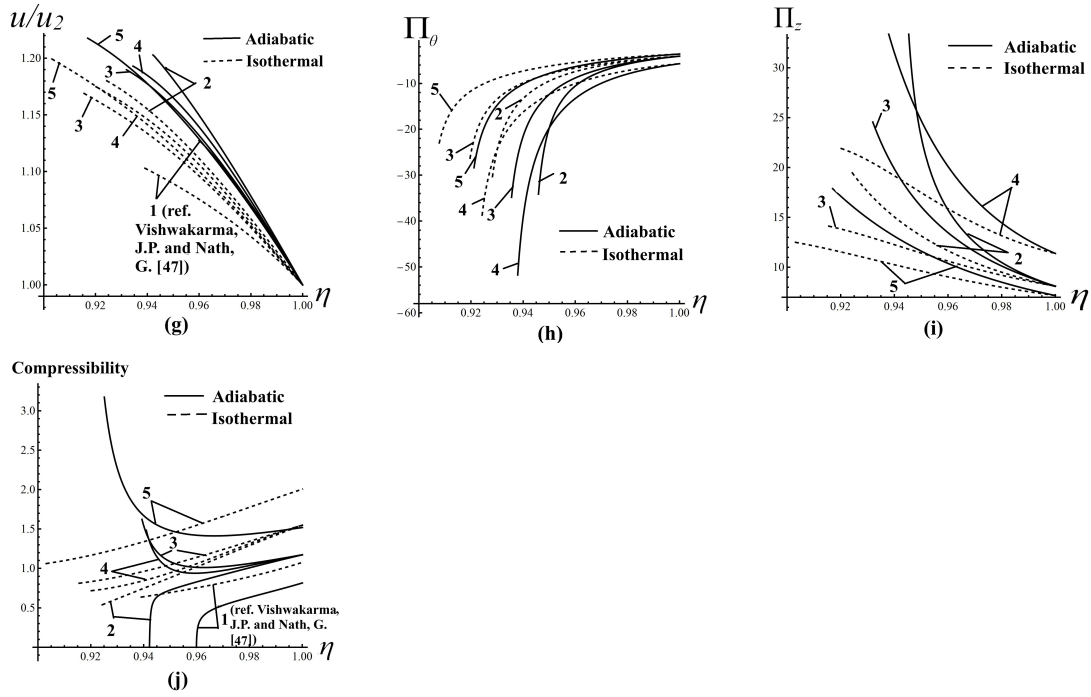

Fig. 2 Continued.

Acknowledgment

G. Nath and Ritika Omar are thankful to the Council of Science & Technology, U.P. (CST, UP), Lucknow for providing financial support to conduct this research via Project ID: 2600, ref. no: CST/D-1522, Dated: 26/10/2023.

References

[1] Ahmad, S., Ullah, A., Shah, K. and Akgü, A., Computational analysis of the third order dispersive fractional PDE under exponential-decay and Mittag-Leffler type kernels, Numer. Methods Partial Differ. Equ., 39 (2023), 4533-4548.

[2] Barkan, A., D'Angelo, N. and Merlino, R. L., Experiments on ion-acoustic waves in dusty plasmas, Planet. Space Sci., 44 (1996), 239–242.

[3] Bilal, M., Ghafoor, A., Hussain, M., Shah, K. and Abdeljawad, T., Numerical scheme for the computational study of two dimensional diffusion and Burgers' systems with stability and error estimate, J. Nonlinear Math Phys., 32 (2025), 1-23.

[4] Blandford, R. and Eichler, D., Particle acceleration a astrophysical shocks: a theory of cosmic ray origin, Phys. Rep., 154 (1987), 1–75.

[5] Carrus, P. A., Fox, P. A., Haas, F. and Kopal, Z., The propagation of shock waves in a stellar model with continuous density distribution, Astrophys. J., 113 (1951), 496–518.

[6] Chaturani, P., Strong cylindrical shocks in a rotating gas, Appl. Sci. Res, 23 (1970), 197–211.

[7] Chefranov, S. G., Dissipative instability of converging cylindrical shock wave, Phys. Fluids, 32 (2020), 114103.

[8] Christer, A. H., Self-similar cylindrical ionizing shock and detonation waves, J. Appl. Math. Mech., 52(1) (1972), 11–22.

[9] Chu, C. K., Dynamics of ionizing shock waves: shocks in transverse magnetic fields, Phys. Fluids, 7(8) (1964), 1349–1357.

[10] Draine, B. T., Physics of the Interstellar and Intergalactic Medium, Princeton University Press, 2011.

[11] Greenspan, H. P., Similarity solution for a cylindrical shock magnetic field interaction, Phys. Fluids, 5(3) (1962), 255-258.

[12] Grover, R. and Hardy, J. W., The propagation of shocks in exponentially decreasing atmospheres, Astrophys. J., 143 (1966), 48–60.

[13] Hartmann, L., Accretion Processes in Star Formation, Cambridge University Press, 1998.

[14] Higashino, F. and Suzuki, T., The effect of particles on blast wave in a dusty gas, Z. Naturforsch., 35 (1980), 1330–1336.

[15] Korobeinikov, V. P., Problems in the theory of point explosion in gases, American Mathematical Society, 1976.

[16] Korobeinikov, V. P., The problem of a strong point explosion in a gas with zero temperature gradient, Dokl. Akad. Nauk SSSR, 109 (1956), 271-273.

[17] Laumbach, D. D. and Probstein, R. F., Self-similar strong shocks with radiations in a decreasing exponential atmosphere, Phys. Fluids, 13(5) (1970), 1178-1183.

[18] Laumbach, D. D. and Probstein, R. F., A point explosion in a cold exponential atmosphere part 2. Radiating flow, J. Fluid Mech., 40 (1970), 833–858.

[19] Levin, V. A. and Skopina, G. A., Detonation wave propagation in rotational gas flows, J. Appl. Mech. Tech. Phys., 45 (2004), 457–460.

[20] Miura, H. and Glass, I. I., Development of the flow induced by a piston moving impulsively in a dusty gas, Proc. Roy. Soc. Lond. A, 397(1813) (1985), 295-309.

[21] Miura, H. and Glass, I. I., On the passage of a shock wave through a dusty gas layer, Proc. R. Soc. London, Ser. A, 385(1788) (1983), 85-105.

[22] Nath, G., Self-similar solutions for unsteady flow behind an exponential shock in an axisymmetric rotating dusty gas, Shock Waves, 24 (2014), 415–428.

[23] Nath, G., Propagation of a strong cylindrical shock wave in a rotational axisymetric dusty gas with exponentially varying density, Res. Astron. Astrophys., 10(5) (2010), 445–460.

[24] Nath, G. and Maurya, A., Similarity solution using optimal classification of Lie subalgebras for shock waves in rotating ideal gas with heat conduction and radiation heat flux under the impact of magnetic field via Lie group analysis, Math. Methods Appl. Sci., 48(17) (2025), 1-32.

[25] Nath, G. and Singh, S., Flow behind magnetogasdynamic exponential shock wave in self-gravitating gas, Int. J. Non-Linear Mech., 88 (2017), 102-108.

[26] Nath, G., Flow behind an exponential shock wave in a perfectly conducting mixture of micro size small solid particles and non-ideal gas with azimuthal magnetic field, Chin. J. Phys., 77 (2022), 2408-2424.

[27] Nath, G., A self-similar solution for the flow behind an exponential cylindrical shock in a self-gravitating mixture of non-ideal gas and a pseudo-fluid of solid particles in a rotating medium, Chin. J. Phys. 84 (2023), 451-470.

[28] Nath, G. and Vishwakarma, J. P., Propagation of a strong spherical shock wave in a gravitating or non-gravitating dusty gas with exponentially varying density, Acta Astronaut., 123 (2016), 200–213.

[29] Nath, G. and Maurya, A., Optimal system of solution using group invariance technique for shock wave in a non-ideal self-gravitating gas in rotating medium in presence of magnetic field, Z. Naturforsch., 78 (2023), 721-742.

[30] Pai, S. I., Menon, S., and Fan, Z. Q., Similarity solution of a strong shock wave propagation in a mixture of a gas and dust particles, Int. J. Eng. Sci., 18(12) (1980), 1365-1373.

[31] Pai, S. I., Two Phase Flows, Vieweg Tracts in Pure Applied Physics Vieweg, Braunschweig, 1977.

[32] Penston, M. V., Dynamics of self-gravitating gaseous spheres—II: Collapses of gas spheres with cooling and the behaviour of polytropic gas spheres, Mon. Not. R. Astron. Soc., 145(4) (1969), 457–485.

[33] Popel, S. I. and Gisko, A. A., Charged dust and shock phenomena in the solar system, Nonlinear Process Geophys., 13(2) (2006), 223-229.

[34] Popel, S. I., Losseva, T. V., Golub, A. P., Merlino, R. L. and Andreev, S. N., Dust ion-acoustic shocks in a Q machine device, Contrib. Plasma Phys., 45 (2005), 461–475.

[35] Popel, S. I., Losseva, T. V., Golub, A. P., Merlino, R. L. and Andreev, S. N., Dissipative processes and dust ion-acoustic shocks in a Q machine device, Phys. Plasmas, 12 (2005), 054501.

[36] Raizer, Y. P., The propagation of a shock wave in a non-homogeneous atmosphere in the direction of decreasing density, Zh. Prikl. Mekh. Tekh. Fiz., 4 (1964), 49–56.

[37] Rao, M. P. R. and Ramana, B. V., Unsteady flow of a gas behind an exponential shock, J. Math. Phys. Sci., 10 (1976), 465–476.

[38] Rosenau, P. and Frankenthal, S., Shock disturbances in a thermally conducting solar wind, Astrophys. J., 208 (1976), 633-670.

[39] Rosenau, P. and Frankenthal, S., Propagation of magnetohydrodynamic shocks in a thermally conducting medium, Phys. Fluids, 21 (1978), 559-566.

[40] Sachdev, P. L. and Ashraf, S., Conversing spherical and cylindrical shocks with zero temperature gradient in the rear flow-field, J. Appl. Math. Phys., 22 (1971), 1095-1102.

[41] Sakurai, A., Propagation of spherical shock waves in stars, J. Fluid Mech., 1(4) (1956), 436–453.

[42] Sakurai, A., Blast Wave Theory, Basic Developments in Fluid Dynamics, Mathematics Research Center, United States Army University of Wisconsin, 1(1964), 101.

[43] Sedov, L. I., Similarity and Dimensional Methods in Mechanics Academic Press, New York, 1959.

[44] Shah, K. and Akram, M., Numerical treatment of non-integer order partial differential equations by omitting discretization of data, Comput. Appl. Math., 37 (2018), 6700-6718.

[45] Solinger, A., Buff, J. and Rappaport, S., Isothermal blast wave model of supernova remnants, Astrophys. J., 201 (1975), 381-386.

[46] Truelove, J. K., Klein, R. I., Mckee, C. F., Holliman II, J., Howell, L. H., Greenough, J. A. and Woods, D. T., Self-gravitational hydrodynamics with three-dimensional adaptive mesh refinement: Methodology and applications to molecular cloud collapse and fragmentation, Astrophys. J., 495(2) (1998), 821–852.

[47] Vishwakarma, J. P. and Nath, G., Similarity solutions for unsteady flow behind an exponential shock in a dusty gas, Phys. Scr., 74(4) (2006), 493–498.

[48] Viswhwakarma, J. P. and Nath, G., Propagation of a cylindrical shock wave in a rotating dusty gas with heat-conduction and radiation heat flux, Phys. Scri., 81 (2010), 045401.

[49] Zel'dovich, Y. B. and Raizer, Y. P., Physics of shock waves and high temperature hydrodynamics phenomena, Academic Press, New York, 1967.

[50] Zhuravskaya, T. A. and Levin, V. A., The propagation of converging and diverging shock waves under intense heat exchange conditions, J. Appl. Math. Mech., 60(5) (1996), 745-752.